Technical Report
RAL-TR-96-103

Consistent Treatment of Charm Evolution in Deep Inelastic Scattering

A D Martin R G Roberts M G Ryskin and W J Stirling

December 1996

COUNCIL FOR THE CENTRAL LABORATORY OF THE RESEARCH COUNCILS

Enquiries about copyright, reproduction and requests for additional copies of this report should be addressed to:

The Central Laboratory of the Research Councils
Library and Information Services
Rutherford Appleton Laboratory
Chilton
Didcot
Oxfordshire
OX11 0QX
Tel: 01235 445384 Fax: 01235 446403
E-mail library@rl.ac.uk

ISSN 1358-6254

DTP/96/102
RAL-TR-96-103
December 1996

Consistent Treatment of Charm Evolution in Deep Inelastic Scattering

A. D. Martin[a], R. G. Roberts[b], M. G. Ryskin[a,c] and W. J. Stirling[a,d]

[a] *Department of Physics, University of Durham, Durham, DH1 3LE*
[b] *Rutherford Appleton Laboratory, Chilton, Didcot, Oxon, OX11 0QX*
[c] *Laboratory of Theoretical Nuclear Physics, St. Petersburg Nuclear Physics Institute, Gatchina, St. Petersburg 188350, Russia*
[d] *Department of Mathematical Sciences, University of Durham, Durham, DH1 3LE*

Abstract

We present a formulation which allows heavy quark $(c, b, \ldots)$ mass effects to be explicitly incorporated in both the coefficient functions and the splitting functions in the parton evolution equations. We obtain a consistent procedure for evolution through the threshold regions for $c\bar{c}$ and $b\bar{b}$ production in deep inelastic scattering, which allows the prediction of the charm and bottom quark densities. We use the new formulation to perform a next-to-leading order global parton analysis of deep inelastic and related hard scattering data. We give predictions for the charm components of the proton structure functions F_2 and F_L as functions of x and Q^2. We examine the Q^2 range of validity of the photon-gluon fusion model for $c\bar{c}$ electroproduction. We emphasize the value of a precision measurement of the charm component F_2^c at HERA.

1. Introduction

A very wide range of deep inelastic scattering structure function data can be successfully described in terms of universal quark and gluon distributions satisfying DGLAP (Q^2) evolution equations. While the formalism for light quarks (i.e. $m_q \ll \Lambda_{QCD}$) is on a sound theoretical footing, the treatment of heavy quarks (i.e. $m_q \gg \Lambda_{QCD}$) is more problematic. The reason is that in practice one requires a consistent description which includes both the kinematical regions $Q^2 \sim m_q^2$ and $Q^2 \gg m_q^2$.

The problem of how to treat heavy quark contributions to deep inelastic structure functions has been widely discussed, see for example [1]. It has been brought into focus recently by the very precise $F_2^{ep}(x,Q^2)$ data from HERA. Both the H1 and ZEUS collaborations have measured [2, 3] the charm quark component F_2^c of the structure function at small x and have found it to be a large (approximately 25%) fraction of the total. This is in sharp contrast to what is found at large x, where typically $F_2^c/F_2 \sim O(10^{-2})$ [4]. Since the HERA F_2 data [6, 7] are a potentially valuable source of information on the gluon distribution, the value of α_S, and the relation between the non-perturbative (low Q^2) and perturbative (high Q^2) domains, it is important that charm component is treated correctly.

In this paper we present a new, theoretically consistent method for calculating the heavy quark contributions to the deep inelastic electroproduction structure functions F_2 and F_L.[1] Our main focus is on the charm quark contribution, although our results apply equally well for bottom and top quarks. The most important feature of our analysis is that it is applicable both to the threshold region $Q^2 \sim 4m_c^2$, where phase space effects are important, and to the asymptotic region $Q^2 \gg 4m_c^2$, where the charm quark assumes the role of a massless parton and the DGLAP resummation of leading $(\alpha_S \ln Q^2)^n$ contributions is necessary.

Before describing our formalism and presenting quantitative predictions, we briefly review existing techniques for treating the charm quark contribution to F_2. The most simplistic approach is to assume that a probe of virtuality Q^2 can resolve a charm quark pair in the proton sea when $Q^2 \gtrsim m_c^2$. Since such pairs originate from fluctuations of the gluon field, $g \to c\bar{c}$, a perturbative treatment should be valid as long as $m_c^2 \gg \Lambda_{QCD}^2$. As Q^2 increases, $O(m_c^2/Q^2)$ corrections to the standard DGLAP evolution become less important, and the charm quark can be treated as a (fourth) massless quark. These ideas are embodied in the 'massless parton evolution' (MPE) approach

$$\begin{aligned} c(x,Q^2) &= 0 \quad \text{for} \quad Q^2 \le \mu_c^2 \,, \\ n_f &= 3 + \theta(Q^2 - \mu_c^2) \quad \text{in} \quad P_{qg},\, P_{gg},\, \beta_0, \ldots \,, \end{aligned} \tag{1}$$

where $\mu_c = O(m_c)$. The charm contribution to the structure function is then

$$F_2^c(x,Q^2) = \tfrac{8}{9} x c(x,Q^2) \tag{2}$$

[1] Note that we only consider here the case of neutral current deep inelastic scattering. The case of charged current scattering, e.g. $W^- c \to s$, will be somewhat different but can in principle be treated using the same techniques.

in lowest order. This is the approach adopted at NLO in the MRS (and CTEQ) global parton analyses, with μ_c chosen to achieve a satisfactory description of the EMC F_2^c data [4]. For example, in the MRS(A) analysis [5] it was found that $\mu_c^2 = 2.7$ GeV^2 and that this was to a good approximation equivalent to taking

$$2c(x,Q_0^2) \;=\; \delta\mathcal{S}(x,Q_0^2) \tag{3}$$

with $\delta \approx 0.02$ at the input scale $Q_0^2 = 4$ GeV^2. That is at the input scale, charm $(c+\bar{c})$ was found to have approximately the same shape as the total quark sea distribution $\mathcal{S}$, and moreover to form about 2% of its magnitude. The input parameter μ_c^2 (or equivalently δ) was chosen to give a good description of the EMC F_2^c data.

Although phenomenologically successful, the MPE model clearly cannot give a precise description of the charm contribution in the threshold region. Two-body kinematics imply that an on-shell $c\bar{c}$ pair can be created by photon-gluon fusion (PGF) provided

$$W^2 = Q^2\frac{1-x}{x} \geq 4m_c^2 \tag{4}$$

where W is the $\gamma^* g \to c\bar{c}$ centre-of-mass energy. That is, at small x, $c\bar{c}$ production is not forbidden even at small $Q^2 < \mu_c^2$ where the MPE approach gives zero[2]. In the PGF approach, which was used, for example, in refs. [9, 10, 11], F_2^c is calculated using the exact matrix elements and phase space for the process $\gamma^* g \to c\bar{c}X$. In leading order in α_S we have

$$F_2^c(x,Q^2) = \int dz\; C_g(z,Q^2,\mu^2)\,\frac{x}{z}\,g\left(\frac{x}{z},\mu^2\right). \tag{5}$$

Note that the scale μ^2 at which the gluon distribution and the coupling α_S (in the coefficient function C_g) are evaluated is not specified at leading order, but one might guess that $\mu^2 = O(m_c^2)$ was appropriate. We discuss a reasonable choice of μ^2 in more detail in section 3 together with the effects coming from next-to-leading order (NLO) corrections. In contrast to the situation for massless quarks, there is no collinear divergence in the leading-order $\gamma^* g \to c\bar{c}$ calculation: the integral over the transverse momentum of the produced $c\bar{c}$ pair is regulated by the quark mass: $\int dk_T^2 k_T^2/(k_T^2+m_c^2)^2$. However, this in turn means that at very high Q^2 the leading-order contribution behaves as $F_2^c \sim \alpha_S(\mu_c^2)\ln(Q^2/m_c^2)$. Higher-order corrections also behave as $(\alpha_S \ln(Q^2/m_c^2))^n$, and fixed-order perturbation theory breaks down. In fact these large logarithms are precisely those which are resummed by the DGLAP evolution equations. Thus at large Q^2 we have to include the charm quark as a parton in DGLAP evolution. The exact next-to-leading order corrections to the PGF structure function are known [12], but, of course, these are not sufficient to provide the whole $(\alpha_S \ln(Q^2/m_c^2))^n$ resummation.

Our goal is to include the charm quark in parton evolution in a consistent way. First, in section 2, we discuss how to include the heavy quark mass in the Altarelli-Parisi splitting

[2] In Ref. [8] the MPE model was modified by the introduction of a smooth 'smearing' function which gave a gradual onset of the charm distribution from a low input scale Q_0^2, namely $Q_0^2 = 1$ GeV^2.

kernels in such a way as not to destroy the original parton interpretation, that is to ensure energy-momentum conservation etc. Interestingly we find that the threshold for the onset of the charm distribution is $Q^2 = 4m_c^2$. Then in section 3 we discuss the coefficient functions. The PGF contribution will be included in the coefficient function for the gluon distribution. Thus below the threshold of the charm distribution, $Q^2 < 4m_c^2$, our result for $c\bar{c}$ production will not be zero but will agree with the PGF approach. However, at large Q^2, as was noted in ref. [13], part of the PGF cross section is automatically generated by the evolution of the charm distribution. To avoid double counting we must therefore subtract from the coefficient function given by PGF the contribution which is generated by evolution in this way. As a consequence, above the charm threshold a smaller and smaller fraction of F_2^c will come from the direct photon-gluon fusion mechanism, and instead the main part will be generated by conventional parton evolution. In section 4 we use the new formulation to perform a NLO global analysis of deep inelastic and related hard scattering data. We find an excellent overall description with, in particular, a significant charm component of F_2 in the HERA regime. The analysis allows us to predict universal charm and bottom quark distributions, $c(x,Q^2)$ and $b(x,Q^2)$. In section 5 we present the partonic decomposition of F_2^c as a function of Q^2 and, for completeness, compare the PGF model estimates. We also give predictions for F_2^b. In section 6 we study the charm component of the longitudinal structure function F_L. Finally, in section 7, we give our conclusions.

2. The effects of the charm mass on evolution

As mentioned above, our aim is to develop the appropriate formalism to describe deep inelastic scattering which incorporates the production of a heavy quark pair (which for definiteness we take to be $c\bar{c}$) and which allows a universal charm parton distribution to be obtained from an analysis of these and other data. We can identify the charm mass effects in the structure functions $F_{2,L}^c$ which describe such scattering from the following subset of integrations[3]

$$\ldots \int \frac{dk_{Ti-1}^2}{k_{Ti-1}^2} \int \frac{dk_{Ti}^2\, k_{Ti}^2}{(k_{Ti}^2+m_c^2)^2} \int \frac{dk_{Ti+1}^2}{k_{Ti+1}^2} \ldots \tag{6}$$

where k_{Ti} are the transverse momenta of the t channel partons. The mass of the charm quark enters in the k_{Ti}^2 integration which results from the $g \to c\bar{c}$ transition, see Fig. 1. For the example of the parton chain shown in Fig. 1 it appears that m_c^2 should also have been retained in the integration over k_{Ti+1}^2. However, we show below that this is only needed at next-to-next-to-leading order (NNLO) in α_S.

First we recall the kinematic regime responsible for the leading-order (LO) result. LO evolution corresponds to the resummation of the leading logarithm terms, $(\alpha_S \ln Q^2)^n$, which arise when the n emitted partons have strongly ordered transverse momenta ($\ldots \ll k_{Ti-1}^2 \ll k_{Ti}^2 \ll$

[3]The general structure of the integrands is $k_T^2/(\text{propagator})^2$, which for massless partons $\sim 1/k_T^2$. The k_T^2 in the numerator arises from the spin structure of the parton vertex.

$k^2_{Ti+1} \ldots$). If two of the partons were to have comparable transverse momenta, $k_{Tj} \sim k_{Tj+1}$, then we would lose a $\ln Q^2$ and obtain instead a NLO contribution of the form $\alpha_S(\alpha_S \ln Q^2)^{n-1}$. We may write the Altarelli-Parisi splitting functions

$$P_{ji} = P^{(0)}_{ji} + \alpha_S P^{(1)}_{ji} + \ldots \tag{7}$$

where $P^{(0)}$ is the LO form and $P^{(1)}$ gives the NLO correction. $P^{(1)}$ includes virtual corrections to the vertex and propagators as well as the possibility of producing a second 's channel' parton with comparable transverse momentum.

2.1. LO evolution with charm

On the scale of the Altarelli-Parisi evolution in $\ln Q^2$, we see that to a good approximation

$$\frac{1}{1 + m_c^2/k^2_{Ti}} \approx \theta(k^2_{Ti} - m_c^2), \tag{8}$$

that is the presence of the charm mass simply cuts out the contribution from the region $k^2_{Ti} \lesssim m_c^2$. To be more precise, as may be anticipated for $g \to c\bar{c}$ production, it turns out that the threshold is better represented by $\theta(k^2_{Ti} - 4m_c^2)$, see section 2.2. Thus at LO accuracy we have massless three flavour evolution for $Q^2 < 4m_c^2$ and massless four flavour evolution for $Q^2 > 4m_c^2$; that is due to strong ordering ($k^2_{Ti+1} \gg k^2_{Ti}$) we can neglect the charm mass in the k^2_{Ti+1} integration of Fig. 1. Therefore at LO the singlet evolution equations have the symbolic form

$$\begin{aligned} \dot{g} &= P_{gg} \otimes g + \sum_q P_{gq} \otimes q + P_{gc} \otimes c \\ \dot{q} &= P_{qg} \otimes g + P_{qq} \otimes q \\ \dot{c} &= P_{cg} \otimes g + P_{cc} \otimes c \end{aligned} \tag{9}$$

where $q = u, d, s$ denotes the light quark density functions and c the charm density. We have abbreviated $P^{(0)}$ by P and $\dot{f} = (2\pi/\alpha_S)\partial f/\partial \ln Q^2$. At LO the quark mass effects are simply encapsulated by

$$P_{ci} = P_{ci}(m_c = 0)\, \theta(Q^2 - 4m_c^2) \tag{10}$$

with $i = g$ or c, and similarly for P_{gc}. Also the virtual contribution to P_{gg} must be modified

$$P_{gg} = \ldots - \frac{1}{3} n_f\, \delta(1 - z) \tag{11}$$

with $n_f = 3 + \theta(Q^2 - 4m_c^2)$, and, of course, we must allow for the increase in the number of active flavours n_f in the running of α_S.

Although we show in (9) only the equation for $\dot{c}$, we note that each heavy quark $(c, b, \ldots)$ requires a separate singlet evolution equation [14] since their splitting functions have different θ function contributions.

2.2. NLO evolution incorporating the charm mass

At NLO the inclusion of quark mass effects is a bit more complicated, although it turns out that we only have to take m_c into account in P_{cg} and then only in the LO part $P_{cg}^{(0)}$. (Of course as a consequence we must adjust the virtual corrections to P_{gg}). The argument is as follows.

We have to improve on approximation (8) of the k_{Ti}^2 integration in (6). To do this we divide the integral into two parts

$$\int \frac{dk_{Ti}^2\, k_{Ti}^2}{(k_{Ti}^2+m_c^2)^2} = \int \frac{d(k_{Ti}^2+m_c^2)}{(k_{Ti}^2+m_c^2)} - \int \frac{m_c^2\, dk_{Ti}^2}{(k_{Ti}^2+m_c^2)^2} \tag{12}$$

where the first term gives the leading logarithm contribution that we discussed in section 2.1. To be specific we have

$$\int_{k_{Ti-1}^2}^{Q^2} \frac{d(k_{Ti}^2+m_c^2)}{(k_{Ti}^2+m_c^2)} = \ln\frac{Q^2}{m_c^2} \tag{13}$$

for $k_{Ti-1}^2 \ll m_c^2$, which is equivalent to the threshold factor $\theta(k_{Ti}^2-m_c^2)$ of (8). The second term in (12), which is concentrated in the region $k_{Ti}^2 \sim m_c^2$, gives a constant contribution. That is, it is a NLO contribution (containing a factor α_S without an accompanying $\ln Q^2$). It means that the m_c^2 effects need only be evaluated in the LO part of the $g \to c\bar{c}$ splitting function, $P_{cg}^{(0)}$. For instance consider the integration over k_{Ti+1} of Fig. 1 and the possibility of m_c^2 effects in P_{cc}. Clearly if $k_{Ti+1}^2 \gg m_c^2$ then the mass terms m_c^2/k_{Ti+1}^2 can be neglected. If, on the other hand, $k_{Ti+1}^2 \sim m_c^2$ then either $k_{Ti}^2 \ll m_c^2$ and $c(x,k_{Ti}^2)=0$ or $k_{Ti}^2 \sim m_c^2$ and we lose two $\ln Q^2$ factors so that the contribution is NNLO, which we omit here. That is, at NLO there are no m_c effects in P_{cc}. A similar argument shows that this is also true for P_{gc}.

In summary, we have shown that at NLO P_{cc} and P_{gc} remain as in section 2.1, whereas

$$P_{cg} = P_{cg}^{(0)}(m_c) + \alpha_S\, P_{cg}^{(1)}(m_c=0)\,\theta(Q^2-4m_c^2). \tag{14}$$

That is we need only evaluate the effect of the charm mass on the LO part of P_{cg}. As a consequence of the change in P_{cg}, we have to adjust the virtual correction to P_{gg} by an amount

$$\Delta P_{gg}^{(0)} = -\delta(1-z)\int_0^1 dz\, z\Big(P_{cg}^{(0)}(z,m_c) - P_{cg}^{(0)}(z,m_c=0)\Big), \tag{15}$$

see section 2.3. This adjustment also restores energy-momentum conservation.

It is straightforward to extend the formalism to allow for charm mass effects in NNLO evolution. We simply need to evaluate the "blocks" $gg \to gg$, $gg \to c\bar{c}$, $q\bar{q} \to c\bar{c}$ to $\mathcal{O}(\alpha_S^2)$ with m_c^2 included explicitly, but only in the region $k_{Ti}^2 \sim m_c^2$. For example, for $gg \to gg$ we would need to evaluate the diagrams shown in Fig. 2.

2.3. Evaluation of quark mass effects in P_{cg}

We note that heavy quark mass effects were studied in refs. [14, 15] in terms of the anomalous dimensions of the moments of structure functions. However, it is difficult to apply the results

to parton evolution, since in these early studies the mass correction plays the role of a higher twist contribution. As a consequence it violates the sum rules which reflect energy-momentum and baryon number conservation.

To restore the partonic picture we use "old fashioned" perturbation theory. That is we calculate the $g \to c\bar{c}$ splitting function P_{cg} in the infinite momentum frame with all three partons on-mass-shell. The parton four momenta are shown in Fig. 3. If the momentum of the gluon is large, $p_g \gg k_T$ and m_c, then the quark momentum is given by

$$k = \left(zp_g + \frac{m_c^2 + k_T^2}{2zp_g}; \quad \boldsymbol{k}_T, zp_g \right), \tag{16}$$

and similarly for k' with $z \to 1-z$ and $\boldsymbol{k}_T \to -\boldsymbol{k}_T$. We may write the probability of the $g \to c\bar{c}$ splitting in the form

$$dw_{cg} = 8g^2 T_R \frac{d^2k_T dk_\parallel}{(2\pi)^3} \left[\frac{1}{(2zp_g)^2\, 2(1-z)p_g} \right] \frac{Sp}{(\Delta E)^2} \tag{17}$$

with colour factor $T_R = \frac{1}{2}$ and where the $[\ldots]$ contain the normalization factors of the two t channel and one s channel quark lines shown in Fig. 3. The energy denominators

$$\Delta E = E_{c\bar{c}} - E_g = \frac{m_c^2 + k_T^2}{2z(1-z)p_g} \tag{18}$$

play the role of the quark propagators and the numerator

$$\begin{aligned} Sp &= \frac{1}{2}\delta_{ab}^{\perp} Tr\left(\gamma_a \frac{\not{k} + m_c}{2} \gamma_b \frac{-\not{k}' + m_c}{2} \right) \\ &= (m_c^2 + k_T^2) \frac{z^2 + (1-z)^2}{2z(1-z)} + m_c^2, \end{aligned} \tag{19}$$

where $\frac{1}{2}\delta_{ab}^{\perp}$ is the average over the two transverse polarizations of the (on mass shell) gluon and $\frac{1}{2}(\not{k} + m_c)$ is the quark density matrix. The factor of 8 in (17) arises from the sum over two polarizations of both the c and $\bar{c}$ and allows for the t channel parton to be either c or $\bar{c}$.

To identify the splitting function we must rewrite (17) in the form

$$dw_{cg} = \frac{\alpha_S}{2\pi} \frac{dz}{z} \frac{dQ^2}{Q^2} P_{cg}^{(0)}(z, m_c, Q^2) \tag{20}$$

where $dk_\parallel = p_g dz$. The outstanding problem is therefore to determine the scale Q^2 appropriate for k_T^2. The scale Q^2 should be chosen so that it correctly reproduces the timescale of the fluctuations of the gluon into the $c\bar{c}$ pair, that is

$$\Delta t \sim \frac{1}{\Delta E} = \frac{2E_g}{Q^2} \tag{21}$$

where ΔE is given by (18). It follows that the appropriate scale is[4]

$$Q^2 = 2p_g\Delta E = \frac{m_c^2 + k_T^2}{z(1-z)} \tag{22}$$

and hence that

$$P_{cg}^{(0)} = 2T_R \left[(z^2 + (1-z)^2) + \frac{2m_c^2}{Q^2}\right] \theta\left(Q^2 - \frac{m_c^2}{z(1-z)}\right). \tag{23}$$

Recall that here P_{cg} stands for the splitting into both $c(\bar{c})$ and $\bar{c}(c)$. An analogous result for QED may be found in ref. [16]. The θ function represents the threshold ($k_T^2 = 0$) for observing the $c\bar{c}$ pair. We see that even if at small x we have more than enough energy W to create a $c\bar{c}$ pair, $W^2 \simeq Q^2/x \gg m_c^2/z(1-z)$, then it is possible that the resolution Q^2 will be insufficient to observe the pair within the short fluctuation time Δt, that is when $Q^2 < m_c^2/z(1-z)$.

The complete effect of the quark mass in the NLO splitting functions which involve the charm quark is contained in (23). It leads to the following correction to P_{gg}

$$\Delta P_{gg}^{(0)} = -\frac{2}{3} T_R\, \delta(1-z) \sqrt{1 - \frac{4m_c^2}{Q^2}} \left(1 + \frac{2m_c^2}{Q^2}\right) \theta(Q^2 - 4m_c^2), \tag{24}$$

see (15).

3. Coefficient functions for deep inelastic charm production

Just as for light quarks, the contribution of charm to the deep inelastic structure function F_2 is obtained from a convolution of the parton distributions and the coefficient functions. We have

$$F_2^c(x,Q^2) = \frac{8}{9}\int_x^1 dz\, \frac{x}{z} \left[C_{q=c}(z,Q^2,\mu^2)\, c\left(\frac{x}{z},\mu^2\right) + C_g(z,Q^2,\mu^2)\, g\left(\frac{x}{z},\mu^2\right)\right] \tag{25}$$

where, due to the quark mass, the coefficient functions have an explicit dependence on Q^2. The charm quark coefficient function in (25) has the form

$$C_c = C_c^{(0)} + \frac{\alpha_S}{4\pi} C_c^{(1)} + \ldots, \tag{26}$$

while for the gluon we have

$$C_g = \frac{\alpha_S}{4\pi} C_g^{(1)} + \ldots. \tag{27}$$

At NLO accuracy, to which we are working, we need only the coefficient functions that are shown explicitly in (26) and (27).

We see that at low scales below partonic threshold, $Q^2 < 4m_c^2$, where $c(x,Q^2) = 0$, the structure function F_2^c is described entirely by γg fusion, that is by the $C_g \otimes g$ convolution.

[4]The same scale was used in the computations of the NLO part of the splitting functions, $P_{ji}^{(1)}$, for the light (massless) quarks.

However, we will find that as Q^2 increases from the charm threshold the contribution from the γc interaction, $C_c \otimes c$, increases rapidly and soon becomes dominant. Of course, as we have already mentioned in the introduction, when the number of active flavours increases from 3 to 4 (as we pass through the threshold region) we must take care to avoid double counting. For example, if we were to take the limit in which charm is regarded as a heavy quark, and never a parton, then the entire contribution to F_2 is

$$F_2^c = \frac{\alpha_S}{4\pi} C_g^{PGF} \otimes g \,. \tag{28}$$

We call this fixed (three) flavour approach the photon-gluon fusion (PGF) approximation. From the above discussion it might appear that the PGF approximation, which clearly gives the correct NLO answer for $Q^2 < 4m_c^2$, will dramatically undershoot the true prediction as Q^2 increases above the charm threshold. This is not so, since *part* of the Feynman diagram which is responsible for the important $C_c \otimes c$ parton evolution contribution is contained in $C_g^{PGF} \otimes g$ in the PGF approximation [13]. Thus to avoid double counting we will have to subtract this contribution from $C_g^{PGF} \otimes g$. The consistent treatment of charm mass effects will therefore allow us to quantify the accuracy of the PGF approximation to F_2^c as a function Q^2.

3.1. The charm quark coefficient function for F_2^c

We must specify the coefficient functions for F_2^c that we introduced in (25)-(27). First the LO charm quark coefficient is given by

$$C_c^{(0)}(z,Q^2) = z\,\delta\Big(z - 1/(1+m_c^2/Q^2)\Big)\left(1 + \frac{4m_c^2}{Q^2}\right) \tag{29}$$

where here z is defined with respect to the charm quark

$$z = z_0 = \frac{x}{x'} = \left(1 + \frac{m_c^2}{Q^2}\right)^{-1}. \tag{30}$$

The last equality follows directly from the mass-shell condition $(x'p+q)^2 = m_c^2$ where x' is the fraction of the momentum of the proton that is carried by the struck charm quark, see Fig. 4. The final factor in (29) allows for the F_L component of $F_2 = F_T + F_L$ where

$$\sigma_L/\sigma_T = 4m_c^2/Q^2. \tag{31}$$

Inserting $C_c^{(0)}$ of (29) into (25) gives a contribution to $F_2^c(x,Q^2)$ proportional to $xc(x',Q^2)$ where here the true scale is $\mu^2 = Q^2$. Since we are working to NLO, we may use the massless quark expression for the coefficient $C_c^{(1)}$.

3.2. The gluon coefficient function for F_2^c

We may write the gluon coefficient function, defined in (27), in the form

$$C_g^{(1)} = C_g^{PGF} - \Delta C_g \tag{32}$$

where the PGF expression for F_2 is [17]

$$C_g^{PGF}(z,Q^2) = \left\{\left[z^2 + (1-z)^2 + \frac{4m_c^2}{Q^2}z(1-3z) - \frac{8m_c^4}{Q^4}z^2\right]\ln\frac{1+\beta}{1-\beta} + \left[8z(1-z) - 1 - \frac{4m_c^2}{Q^2}z(1-z)\right]\beta\right\}\theta\left(Q^2\left(\frac{1}{z}-1\right) - 4m_c^2\right). \quad (33)$$

β is the velocity of one of the charm quarks in the photon-gluon centre-of-mass frame

$$\beta^2 = 1 - \frac{4m_c^2 z}{Q^2(1-z)}. \quad (34)$$

The θ function in (33), $\theta(W^2 - 4m_c^2)$, represents the $c\bar{c}$ production threshold, where W is the c.m. energy. Its presence guarantees $\beta^2 \geq 0$. The ΔC_g term in (32) is necessary to avoid the double counting of the graph that we have already used to compute $P_{cg}^{(0)}$, see section 2.3. That is we must subtract from C^{PGF} the term $P_{cg}^{(0)} \otimes C_c^{(0)}$ that we already include in the parton evolution up to Q^2. The z variable in the gluon coefficient functions is defined with respect to the gluon momentum fraction x_g,

$$z = \frac{x}{x_g} = z_0 z' \quad (35)$$

where $z' = x'/x_g$, see Fig. 4. Thus the explicit form of the subtraction term is

$$\Delta C_g(z,Q^2) = \theta\left(Q^2\left(\frac{1}{z}-1\right) - 4m_c^2\right)\int\frac{dz_0}{z_0}C_c^{(0)}(z_0,Q^2)\int_{Q^2_{min}}^{Q^2} d\ln Q'^2\, P_{cg}(z',Q'^2)$$
$$= \theta\left(Q^2\left(\frac{1}{z}-1\right) - 4m_c^2\right)\left(1 + \frac{4m_c^2}{Q^2}\right)\int_{Q^2_{min}}^{Q^2} d\ln Q'^2\, P_{cg}(z',Q'^2) \quad (36)$$

where the θ function reflects the energy threshold $W^2 > 4m_c^2$. The lower limit of integration is given by the "resolution" θ function which is hidden in $P_{cg}(z',Q'^2)$. From (23) we have

$$Q^2_{min} = \frac{m_c^2}{z'(1-z')} \quad (37)$$

where $z' = z/z_0 = (1 + m_c^2/Q^2)z$. The integration in (36) may be readily performed to give

$$\Delta C_g(z,Q^2) = \left[\left\{z'^2 + (1-z')^2\right\}\ln\left(z'(1-z')\frac{Q^2}{m_c^2}\right) + 2z'(1-z') - \frac{2m_c^2}{Q^2}\right]\left(1 + \frac{4m_c^2}{Q^2}\right), \quad (38)$$

where we require both $Q^2 > Q^2_{min}$ and $Q^2 > 4m_c^2 z/(1-z)$.

It is interesting to consider the $m_c^2 \to 0$ limits of C_g^{PGF} and ΔC_g. We have

$$C_g^{PGF} \to \left\{z^2 + (1-z)^2\right\}\ln\left(\frac{1-z}{z}\frac{Q^2}{m_c^2}\right) + 8z(1-z) - 1 \quad (39)$$

as $m_c \to 0$, which differs from the exact $m_c = 0$ coefficient $C_g^{(1)}$ by the presence of Q^2/m_c^2 in the argument of the logarithm. However, from (38) we see that

$$\Delta C_g \to \left\{z^2 + (1-z)^2\right\} \ln\left(z(1-z)\frac{Q^2}{m_c^2}\right) + \ldots \tag{40}$$

as $m_c \to 0$, which removes the $\ln(Q^2/m_c^2)$ term in $C_g^{(1)} = C_g^{PGF} - \Delta C_g$. In C_g^{PGF} the logarithm also comes after an integration over Q'^2 but with a cut-off due to the $\theta(W^2 - 4m_c^2)$ function, as compared to the lower cut-off in (36) arising from the resolution θ function, $\theta(Q^2 - m_c^2/z'(1-z'))$. In the case of light quarks with $m_q \to 0$ neither of these θ functions gives the lower limit; rather it is provided by the confinement scale $Q'^2 > Q_0^2 \gg m_q^2$.

We now come to the choice of the scale μ^2 in the gluon convolution contribution in (25). In the absence of a complete NNLO calculation, which would introduce terms compensating the variation with scale, we must attempt to identify the 'natural' scale for the process. We have already mentioned that the natural scale for the charm convolution is $\mu^2 = Q^2$. In the pure PGF approach the integration over dQ'^2 starts from $Q'^2 \sim m_c^2$ and so a reasonable choice of scale is $\mu^2 = m_c^2$ [10]. However, the region $Q'^2 \ll Q^2$ in C_g^{PGF} is cancelled by the subtraction term ΔC_g so the appropriate choice of scale in $C_g \otimes g$ is $\mu^2 \sim Q^2$. The $\mathcal{O}(\alpha_S^2)$ corrections to PGF have been computed by Laenen et al. [12] and found to be significant, particularly at larger x values. In an attempt to roughly reproduce this NNLO contribution we find that it is better to take $\mu^2 \sim Q^2/4$. This is not unexpected since the Q^2 of the photon probe has to be shared between the two vertices of the quark box. Of course at small Q^2 when $Q^2/4 < m_c^2$ we should revert to $\mu^2 = m_c^2$. Thus for the $C_g \otimes g$ contribution to F_2^c we take the scale $\mu^2 = \max\{Q^2/4, m_c^2\}$.

4. Charm as a parton in a global analysis

The measurements of F_2 at HERA have become much more precise with errors as small as $\pm 3\%$ or less. Moreover, since the charm component F_2^c of F_2 is about 0.25 in the HERA regime it is important to improve the treatment of charm in the analysis of deep inelastic scattering data. This was the objective of sections 2 and 3 above. The new formalism incorporates the heavy quark masses in the parton evolution equations and allows a determination of the (universal) charm and bottom quark densities. Indeed we can predict $c(x, Q^2)$ and $b(x, Q^2)$, as well as the charm and bottom components of F_2, directly from a knowledge of the gluon and other quark densities. There are no free parameters, although the results do depend on the values of m_c and m_b, and, as usual, on the truncation of the perturbation expansion. As in previous analyses, we work to NLO.

The new framework is a significant advance on the existing treatment of charm in deep inelastic scattering. Recall that two different types of approach are used at present. In the first, charm is set to zero below some scale ($c(x, Q^2) = 0$ for $Q^2 < \mu^2$) and for $Q^2 > \mu^2$ the charm distribution is evolved assuming that $m_c = 0$. Although this procedure is clearly inaccurate in the $c\bar{c}$ threshold region, the parameter μ is chosen so that the fixed-target F_2^c data are well

described. Secondly, we have the PGF approach [10, 11] based on the calculation of $\gamma^* g \to c\bar{c}$ with the correct kinematics, but in which c is not treated as a parton. As we have seen, this gives the correct description of F_2^c for $Q^2 < 4m_c^2$ and should remain a reasonable approximation to F_2^c for $Q^2 \gtrsim 4m_c^2$. However, the PGF model will inevitably break down at larger Q^2 values when charm can no longer be treated as a non-partonic heavy object and when it begins to evolve more like the lighter components of the quark sea.

Before we present our predictions for $c(x,Q^2)$ and $b(x,Q^2)$, we perform a NLO global analysis of deep inelastic and related data which incorporates the $m_q \neq 0$ parton evolution procedure that we introduced in sections 2 and 3. This may be regarded as a small refinement of the global analysis determination of the gluon and light quark densities of ref. [8], but it does allow the gluon (and other parton) distributions to readjust themselves to accommodate the new treatment of $c(x,Q^2)$. Recall that the heavy quark distributions, $c(x,Q^2)$ and $b(x,Q^2)$, do not contain any free parameters apart, of course, from m_c and m_b. Motivated by QCD sum rules, we take $m_c = 1.35$ GeV and $m_b = 4.3$ GeV [18]. We show the effects of varying the value of m_c when we discuss the description of F_2^c. In fact we find that the overall description of the data (and in particular of F_2 in the HERA regime) improves compared to our previous analyses [8]. The only change to the data set that we use is the addition of the final NMC data [19] for F_2.

We shall present full details of the new global analysis [5] in a future paper in which we will discuss the improvements of the deep inelastic data and their implications. However, in Table 1 we illustrate the quality of the new fit relative to our previous fit that best described the HERA data, MRS(R2) [8].

Experiment	# data	χ^2	
		MRRS	MRS(R_2)
H1 F_2^{ep}	193	127	149
ZEUS F_2^{ep}	204	280	308
BCDMS $F_2^{\mu p}$	174	287	320
NMC $F_2^{\mu p}$	130	145	134
NMC $F_2^{\mu d}$	130	119	98
E665 $F_2^{\mu p}$	53	60	62
SLAC F_2^{ep}	70	91	95

Table 1: χ^2 values for some of the data [6,7,18,19,20,21] used in the global fit. Note the larger χ^2 values for the E665 points [21] than those quoted in ref. [8] — these result from our correcting our previous incorrect treatment of the E665 experimental errors.

[5] The FORTRAN code for this set of partons, MRRS, together with the code for computing each flavour component to F_1, F_2 and F_L is available by electronic mail from `W.J.Stirling@durham.ac.uk`, or directly from `http://durpdg.dur.ac.uk/HEPDATA/MRS`.

The HERA data lie in the region where F_2^c/F_2 is largest and there is clear improvement in the new fit for these data. The value of α_S resulting from the new fit is $\alpha_S(M_Z^2) = 0.116_4$, intermediate to the values 0.113 and 0.120 of MRS(R1) and (R2) and the lower χ^2 for the BCDMS data in the Table is due to this. Our prescription for $\alpha_S(Q^2)$ across charm and bottom thresholds is to match the values at $Q^2 = 4m_c^2$, and again at $Q^2 = 4m_b^2$. Thus we define

$$\alpha_{S(4)}(Q^2) = \alpha_S(Q^2, 4) \tag{41}$$

and take, for 5 flavours,

$$\alpha_{S(5)}^{-1}(Q^2) = \alpha_S^{-1}(Q^2, 5) + \alpha_S^{-1}(4m_b^2, 4) - \alpha_S^{-1}(4m_b^2, 5), \tag{42}$$

while for 3 flavours we have

$$\alpha_{S(3)}^{-1}(Q^2) = \alpha_S^{-1}(Q^2, 3) + \alpha_S^{-1}(4m_c^2, 4) - \alpha_S^{-1}(4m_c^2, 3). \tag{43}$$

In Fig. 5 we show the flavour decomposition of the sea as a function of Q^2 for two different values of x. Recall that there are now no input parameters for the heavy quark distributions, $c(x, Q^2)$ and $b(x, Q^2)$, and that they are determined in terms of the gluon (and other parton) distributions.

We show the description of both the fixed target and HERA data for F_2^c in the next section. The charm data are not used in the global fit. However, when they become more precise these data should be included as they will provide a significant extra constraint on the gluon distribution. The gluon density from the new fit compares very closely with that of MRS(R2). The new gluon is more 'valence-like' at $Q_0^2 = 1$ GeV^2, but for $Q^2 \geq 2$ GeV^2 both gluon distributions rise at small x and become increasingly similar as Q^2 continues to increase.

5. The structure of F_2^c

Fig. 6 shows the partonic decomposition of F_2^c as given by (25), which may be written in the symbolic form

$$F_2^c = C_c \otimes c + C_g \otimes g. \tag{44}$$

The gluonic component gives the total production below the charm threshold, $Q^2 < 4m_c^2$. However, the component driven by the charm distribution rises rapidly above threshold and becomes dominant at larger Q^2. We also show for comparison the photon-gluon fusion prediction $C^{PGF} \otimes g$. The PGF model and our prediction are identical below threshold, $Q^2 < 4m_c^2$. Above threshold we see that the rapid onset of the charm parton component $C_c \otimes c$ is largely balanced by the subtraction ΔC_g from the PGF result. Nevertheless, as we would expect, the compensation is not exact and the inclusion of the evolution of charm does result in a larger value of F_2^c above the threshold, see Fig. 6. By $Q^2 = 100$ GeV^2, for example, for $x = 0.05$ (0.005) the improved description, in which charm is treated as a parton, lies some 33% (18%) above the PGF model. The approximately constant behaviour of $C_g \otimes g$ seen in Fig. 6 for

$Q^2 \gtrsim 50$ GeV^2 may be anticipated. In this kinematic regime the gluon is approximately scaling and the m_c^2/Q^2 terms in C_g are small. Moreover, there are no $\ln Q^2/m_c^2$ terms in C_g after the ΔC_g subtraction. The lack of smoothness in the prediction for F_2^c, apparent in Fig. 6 in the threshold region, is a consequence of assuming that the threshold for the resolution of charm can be exactly described by a θ function. More realistically, the onset of charm will be smeared out around $Q^2 = 4m_c^2$ leading to a much smoother behaviour, although such smearing will have a negligible effect on the global analysis.

The comparisons of the predictions for F_2^c with the EMC and the HERA data are shown in Fig. 7. The overall agreement over quite an extensive range of x and Q^2 is good. The dotted and dashed curves in Fig. 7 show the effect of taking $m_c = 1.2$ and 1.5 GeV respectively, rather than the central value, $m_c = 1.35$ GeV, which we use throughout this paper.

Fig. 8 shows the fraction of charm deep inelastic events as a function of Q^2 for selected values of x. The strong production of charm at HERA is evident; moreover we see a sensitive dependence on x and Q^2. If a significant fraction of the numerous charm events can be cleanly isolated in the experiments at HERA then the resulting precision measurement of F_2^c, coupled with the measurement of F_2, will provide a powerful double constraint on the gluon distribution, as well as offering a stringent scheme independent test of QCD along the lines of that using F_2 and F_L proposed by Catani [23].

6. Predictions for F_L^c

We may also use the new formalism which incorporates the quark mass to calculate the charm component F_L^c of the longitudinal structure function. We use expressions that are identical to (25)–(27) and (32) but with the coefficient functions $C_{q=c}$ and C_g that are appropriate to F_L^c. For the quark coefficient we have

$$C_c^{(0)} = \frac{4m_c^2}{Q^2}\, z\, \delta\left(z - (1 + m_c^2/Q^2)^{-1}\right), \tag{45}$$

whereas for $C_c^{(1)}$ we may use the massless quark expression, since we are working to NLO accuracy. For the gluon coefficient for F_L^c we have

$$C_g^{(1)} = C_g^{PGF} - \Delta C_g \tag{46}$$

where

$$C_g^{PGF}(z, Q^2) = 4\beta\, z(1-z) - 8z^2\, \frac{m_c^2}{Q^2}\, \ln\frac{1+\beta}{1-\beta} \tag{47}$$

with $Q^2 > 4m_c^2 z/(1-z)$, where the quark velocity β is given by (34). Here the subtraction term is

$$\Delta C_g(z, Q^2) = \frac{4m_c^2}{Q^2}\left[\ldots\right] \tag{48}$$

where $[\ldots]$ is the expression in the square brackets in (38). For ΔC_g to be non-zero we require $Q^2 > Q^2_{min}$ and $Q^2 > 4m_c^2 z/(1-z)$, where Q^2_{min} is given by (37).

In Fig. 9 we present the predictions for F_L in terms of the ratio $R^c = F_L^c/F_T^c$. Due to the factor $4m_c^2/Q^2$ in the coefficient function of the LO charm component given in (45), we have a pronounced peak in R^c just above the partonic threshold, $Q^2 = 4m_c^2$. Clearly R^c will decrease at higher Q^2. The NLO gluonic component gives a smaller value of R^c than the charm component. Hence the peak is more pronounced at larger x when the gluonic component is less important. We also show in Fig. 9 the values of $R = F_L/F_T$.

7. Conclusions

We have determined the charm and bottom quark densities of the proton taking into account the effects of their non-zero mass. In particular we have presented a formalism which incorporates m_c and m_b into the Altarelli-Parisi splitting functions and in the coefficient functions in a consistent way. We can therefore evolve up in Q^2 taking proper account of the heavy quark thresholds. At NLO accuracy we show that the main effect of the quark mass is in the splitting function $P_{cg}^{(0)}$ (or $P_{bg}^{(0)}$).

We showed that the threshold for the charm density, $c(x,Q^2)$, occurs at $Q^2 = 4m_c^2$. On the other hand we know that the threshold for deep inelastic $c\bar{c}$ production is given by $W^2 = 4m_c^2$, or equivalently $Q^2 = 4m_c^2(1-x)/x$, which for small x occurs below the partonic threshold $Q^2 = 4m_c^2$. This apparent contradiction has a simple explanation. In the region $Q^2 < 4m_c^2$ we find that Q^2 is too small to allow sufficient time to observe the $g \to c\bar{c}$ fluctuations which occur within the proton. Here the photon-gluon fusion mechanism, $\gamma^* g \to c\bar{c}$, gives the complete answer. For evolution above the partonic threshold the structure of F_2^c is more interesting. The charm component $\gamma^* c \to c$ with a spectator $\bar{c}$ quark (or vice-versa with $c \leftrightarrow \bar{c}$) increases rapidly and soon exceeds the NLO part of the gluonic contribution $\gamma^* g \to c\bar{c}$. In the partonic description the LO part of the gluon now has the structure $(g \to c\bar{c}) \otimes (\gamma^* c \to c)$. To avoid double counting we must therefore subtract this LO contribution of the gluon and keep only the part coming from $C_g^{(1)}$.

In addition to its importance in determining the charm quark density $c(x,Q^2)$, the correct formulation of charm mass effects in evolution has become essential in order to obtain an accurate description of F_2 in the HERA domain. The reasons are that the charm component of F_2 is appreciable ($F_2^c/F_2 \sim 0.25$ for $x \sim 0.001$ and $Q^2 \sim 25$ GeV^2) and that the measurements of F_2 at HERA are now much more precise.

Acknowledgements

We thank Valery Khoze, Jan Kwiecinski and Robert Thorne for useful discussions. MGR thanks the Royal Society for a Fellowship grant, and for support from the Russian Fund of Fundamental Research 96 02 17994.

References

[1] W.-K. Tung, Proc. of Int. Workshop on Deep Inelastic Scattering and Related Subjects (DIS 94), Eilat 1994, Ed. A. Levy (World Scientific, 1994), p.29.

[2] H1 collaboration: C. Adloff *et al.*, DESY-96-138, July 1996.

[3] ZEUS collaboration: "D^* Production in Deep Inelastic Scattering at HERA", contribution to the XXVIII Int. Conf. on HEP, Warsaw 1996.

[4] EMC collaboration: J.J. Aubert *et al.*, Nucl. Phys. **B213** (1983) 31.

[5] A.D. Martin, R.G. Roberts and W.J. Stirling, Phys. Rev. **D50** (1994) 6734.

[6] H1 collaboration: H1 collaboration: S. Aid *et al.*, Nucl. Phys. **B470** (1996) 3.

[7] ZEUS collaboration: M. Derrick *et al.*, Zeit. Phys. **C69** (1996) 607; preprint DESY 96-076 (1996), to be published in Zeit. Phys.

[8] A.D. Martin, R.G. Roberts and W.J. Stirling, Phys. Lett. **B387** (1996) 419.

[9] M. Glück, E. Hoffmann and E. Reya, Z. Phys. **C13** (1982) 119.

[10] M. Glück, E. Reya and M. Stratmann, Nucl. Phys. **B422** (1994) 37.

[11] A.J. Askew, J. Kwiecinski, A.D. Martin and P.J. Sutton, Phys. Rev. **D47** (1993) 3775; J. Kwiecinski, A.D. Martin and P.J. Sutton, Z. Phys. **C71** (1996) 585.

[12] E. Laernen, S. Riemersma, J. Smith and W.L. van Neerven, Nucl. Phys. **B392** (1993) 162.

[13] M.A.G. Aivazis, J.C. Collins, F.I. Olness and W.-K. Tung, Phys. Rev. **D50** (1994) 3102.

[14] B.J. Edwards and T. Gottschalk, Nucl. Phys. **B196** (1982) 328;
Yu. P. Ivanov, Sov. J. Nucl. Phys. **44** (1986) 317.

[15] T. Gottschalk, Nucl. Phys. **B191** (1981) 227.

[16] V.A. Khoze *et al.*, Nucl. Phys. **B65**(1973) 381.

[17] E. Witten, Nucl. Phys. **B104** (1976) 445;
M.A. Shifman, A.I. Vainshtein and V.I. Zakharov, Nucl. Phys. **B136** (1978) 157;
M. Glück and E. Reya, Phys. Lett. **B83** (1979) 98.

[18] *Review of Particle Physics*, Particle Data Group, R.M. Barnett *et al.*, Phys. Rev. **D54** (1996) 1.

[19] NM Collaboration: M. Arneodo *et al.*, Nucl. Phys. (in press), hep-ph-9610231.

[20] BCDMS collaboration: A.C. Benvenuti *et al.*, Phys. Lett. **B223** (1989) 485.

[21] L.W. Whitlow *et al.*, Phys. Lett. **B282** (1992) 475.
L.W. Whitlow, preprint SLAC-357 (1990).

[22] E665 collaboration: M.R. Adams *et al.*, Phys. Rev. **D54** (1996) 3006.

[23] S. Catani, to be published in Proc. of Workshop on Deep Inelastic Scattering and Related Phenomena (DIS 96), Rome, hep-ph/9608310.

Figure Captions

Fig. 1 Part of the parton chain occurring in the description of deep inelastic scattering which contains the $g \to c\bar{c}$ transition.

Fig. 2 An example of a "block" diagram along the parton chain, which gives NNLO charm mass effects if the two s channel charm quarks have comparable transverse momenta. Then the charm mass should be retained for all the quark lines that are shown.

Fig. 3 The diagram used to calculate the charm mass effects in $P_{cg}^{(0)}$.

Fig. 4 The variables used in the discussion of the coefficient functions $C_{q=c}(z,Q^2)$ and $C_g(z,Q^2)$. For the charm quark function the variable $z = x/x'$, while for the gluon function $z = x/x_g$, see eq. (30) and (35) respectively; x is the usual Bjorken $x \equiv Q^2/2p.q$.

Fig. 5 The flavour decomposition of the quark sea distribution of the proton as a function of Q^2 at two values of x. The total sea is given by $S = 2(\overline{u} + \overline{d} + s + c + b)$.

Fig. 6 The partonic decomposition of F_2^c as a function of Q^2 for $x = 0.05$ and $x = 0.005$. For $Q^2 \leq 4m_c^2/Q^2$ there is only the contribution from $C_g = C_g^{PGF}$. For larger Q^2, $C_g = C_g - \Delta C_g$ and the total F_2^c is the sum of this contribution and that from C_c.

Fig. 7 The description of the EMC and HERA measurements of F_2^c. The solid line corresponds to our new fit with $m_c = 1.35$ GeV. The dashed and dotted lines correspond to taking $m_c = 1.5$ and 1.2 GeV respectively, with all other parameters unchanged.

Fig. 8 The ratios F_2^c/F_2 and F_2^b/F_2 at fixed values of Q^2 resulting from the new global fit (in which we take $m_c = 1.35$ GeV and $m_b = 4.3$ GeV). The experimental data point shows the estimate from ref. [2] for F_2^c/F_2 in the HERA region.

Fig. 9 The predictions for $R^c = F_L^c/F_T^c$ and $R = F_L/F_T$ as a function of Q^2 for $x = 0.0005$ and $x = 0.05$.

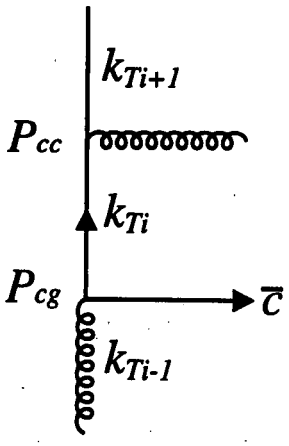

Fig.1

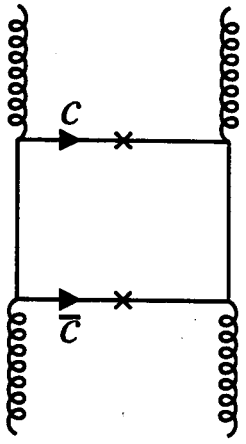

Fig.2

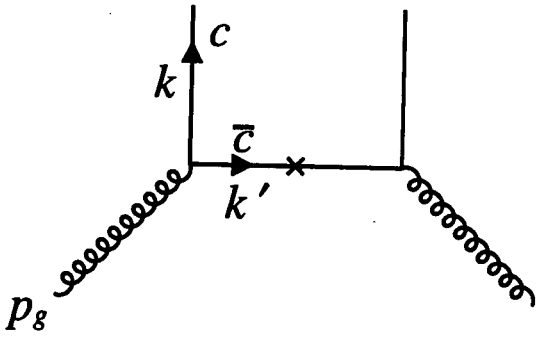

Fig.3

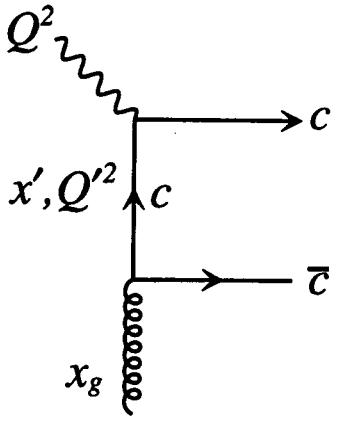

Fig.4

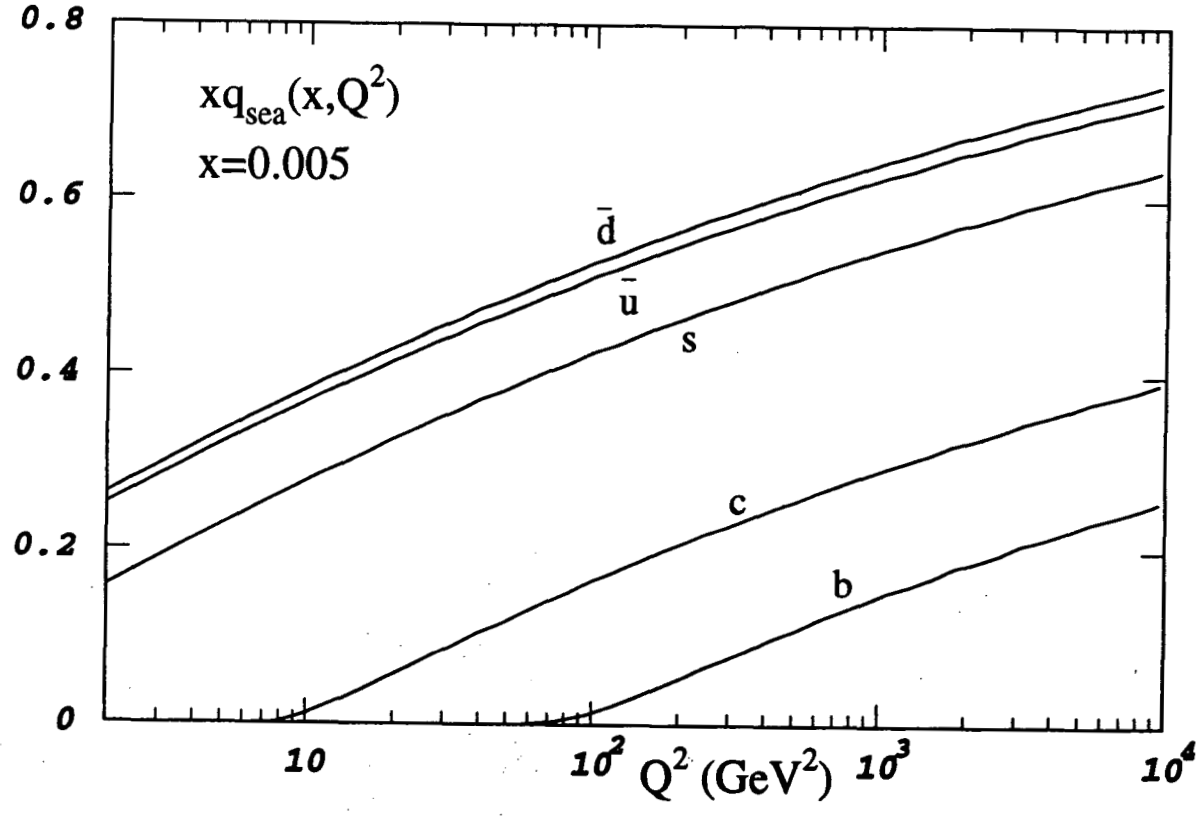
0.8
0.6
0.4
0.2
0
$xq_{sea}(x,Q^2)$
x=0.005
$\bar{d}$
$\bar{u}$
s
c
b
10
10^2
Q^2 (GeV^2)
10^3
10^4

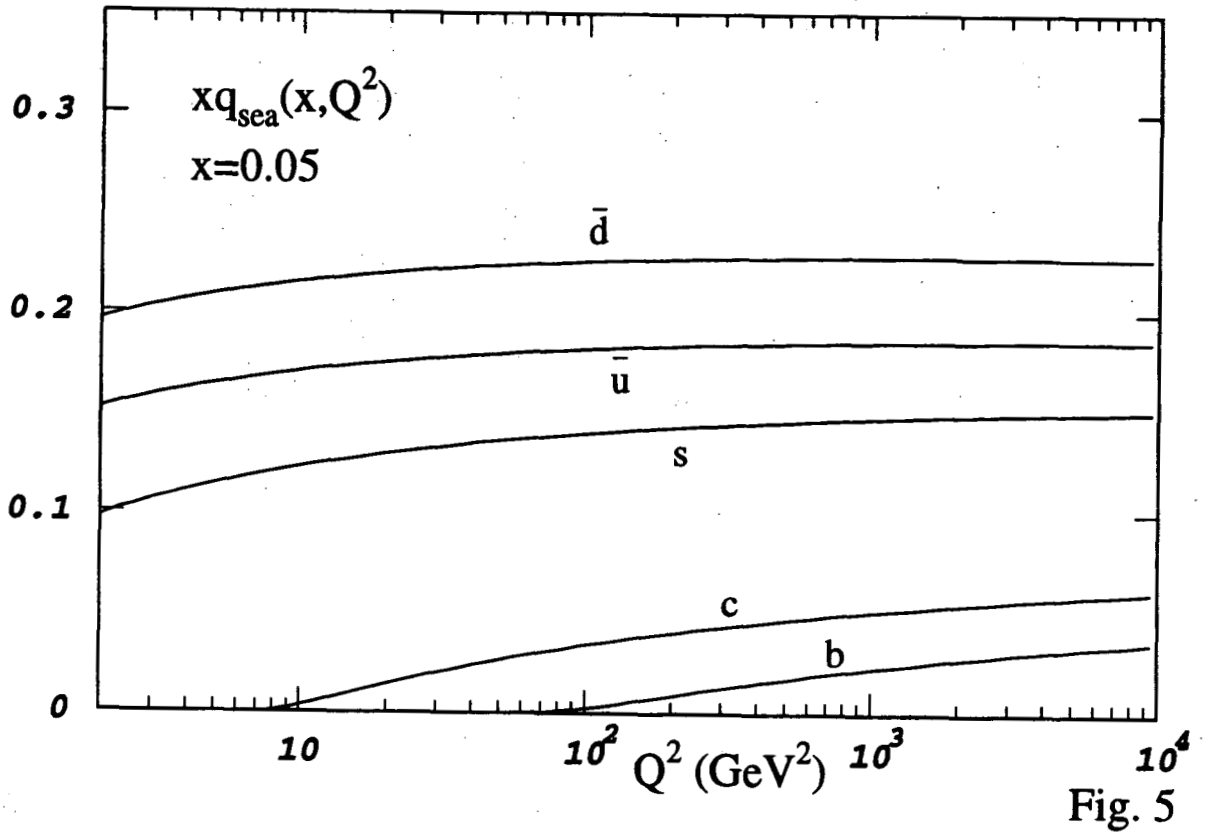
0.3
0.2
0.1
0
$xq_{sea}(x,Q^2)$
x=0.05
$\bar{d}$
$\bar{u}$
s
c
b
10
10^2
Q^2 (GeV^2)
10^3
10^4

Fig. 5

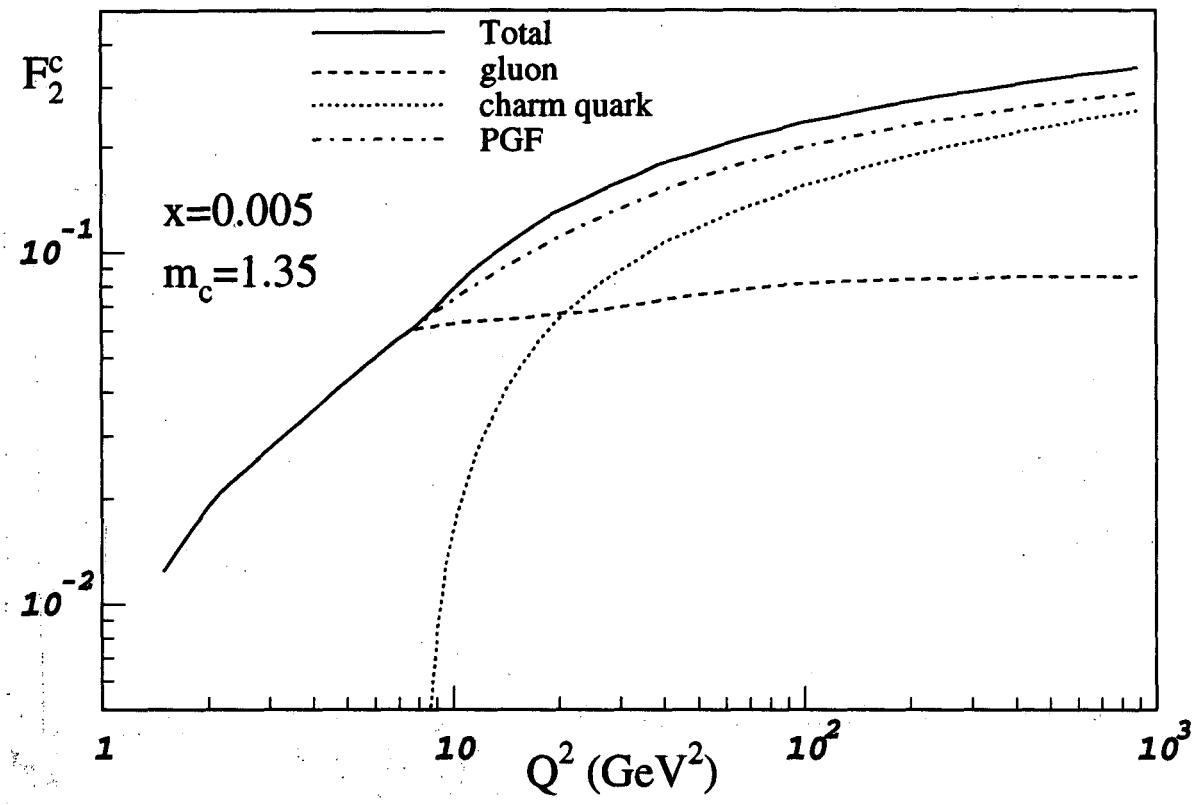
Total
gluon
charm quark
PGF
F_2^c
x=0.005
m_c=1.35
10^{-1}
10^{-2}
1
10
10^2
10^3
Q^2 (GeV^2)

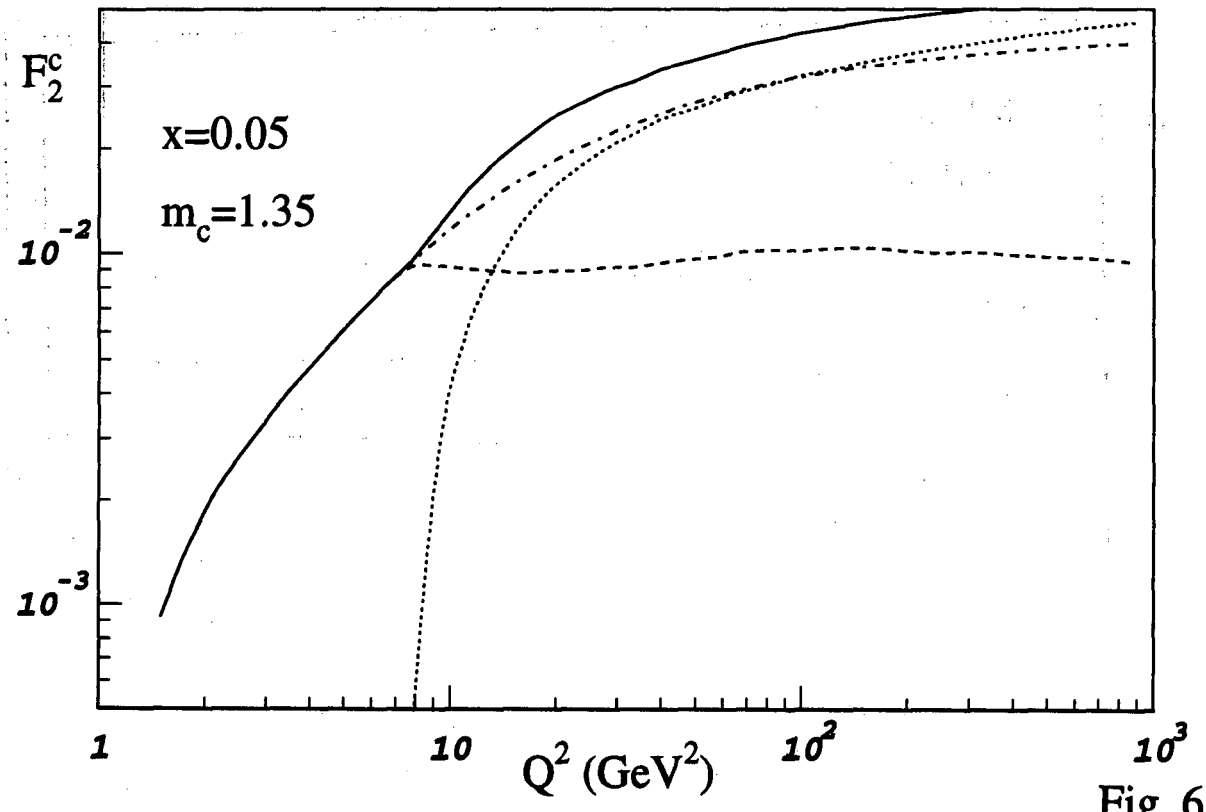
F_2^c
x=0.05
m_c=1.35
10^{-2}
10^{-3}
1
10
10^2
10^3
Q^2 (GeV^2)

Fig. 6

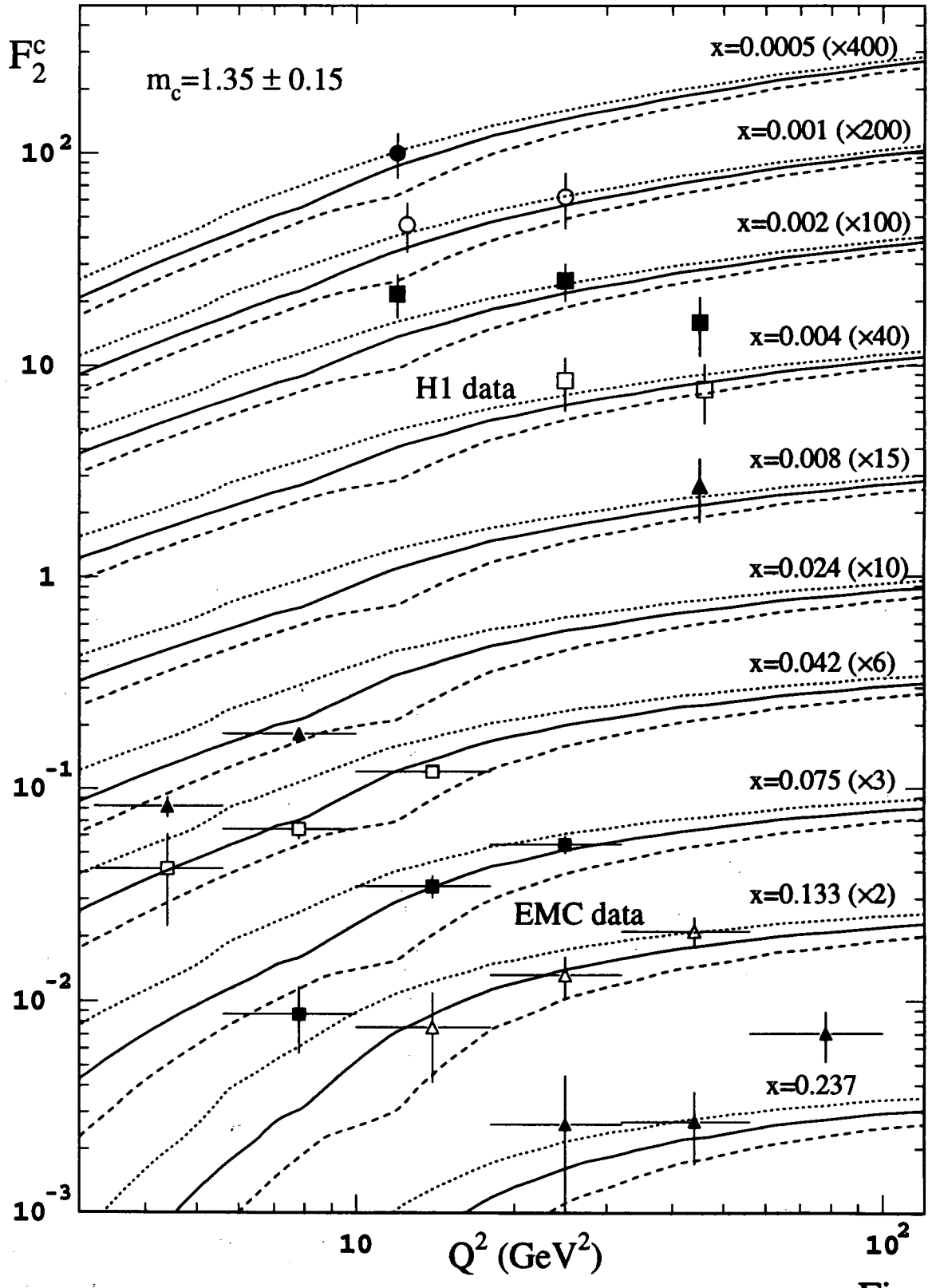
F_2^c
m_c=1.35 ± 0.15
x=0.0005 (×400)
x=0.001 (×200)
x=0.002 (×100)
x=0.004 (×40)
H1 data
x=0.008 (×15)
x=0.024 (×10)
x=0.042 (×6)
x=0.075 (×3)
x=0.133 (×2)
EMC data
x=0.237
10^2
10
1
10^{-1}
10^{-2}
10^{-3}
10
Q^2 (GeV^2)
10^2

Fig. 7

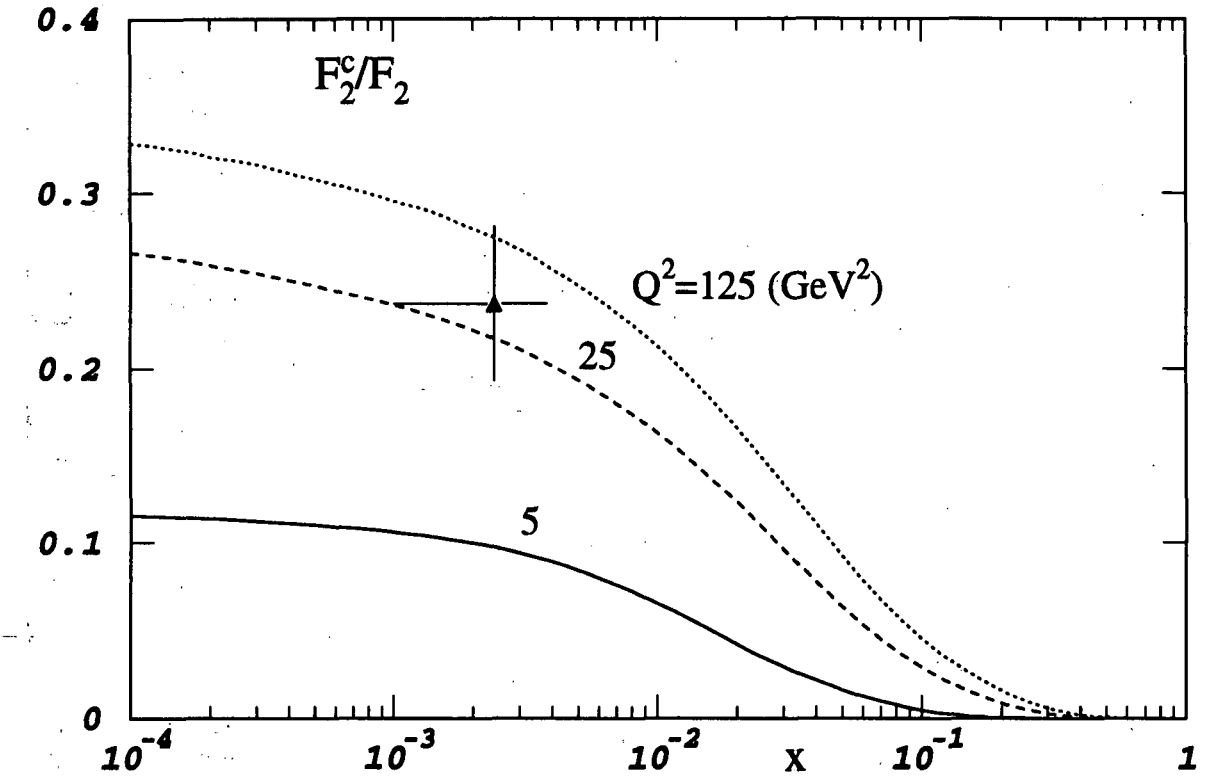
0.4
0.3
0.2
0.1
0
F_2^c/F_2
Q^2=125 (GeV^2)
25
5
10^{-4}
10^{-3}
10^{-2}
x
10^{-1}
1

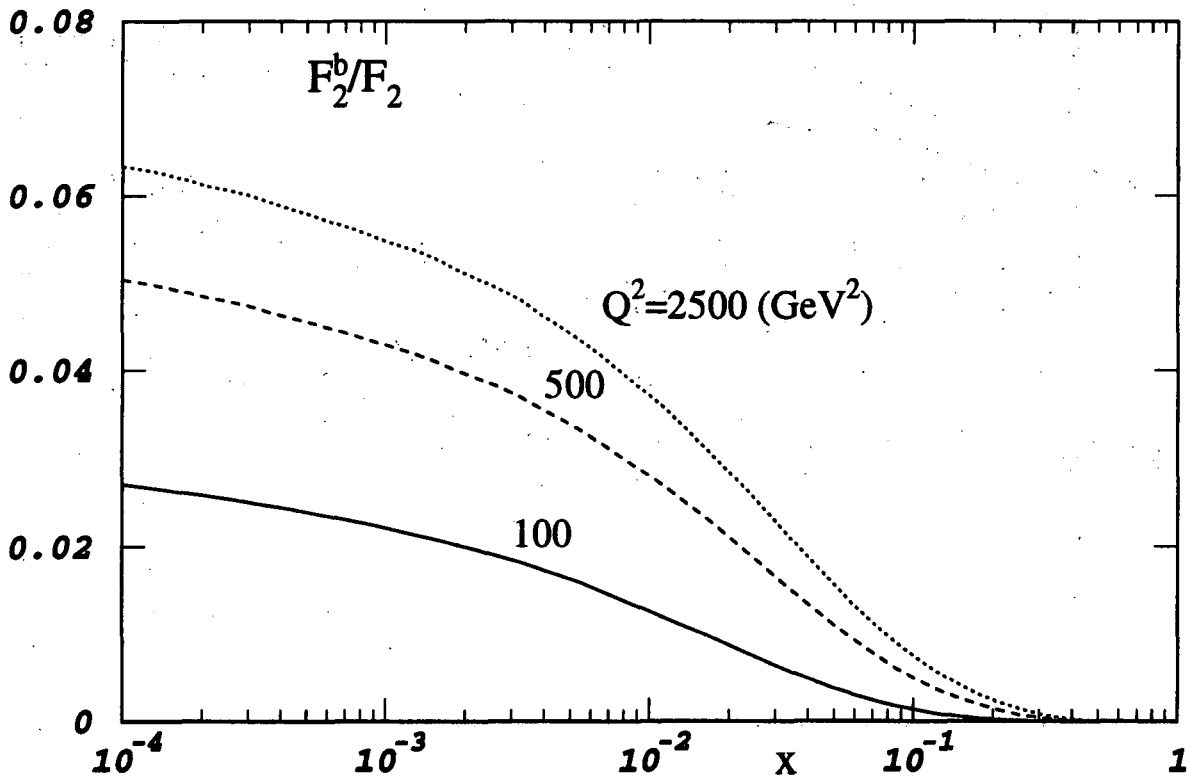
0.08
0.06
0.04
0.02
0
F_2^b/F_2
Q^2=2500 (GeV^2)
500
100
10^{-4}
10^{-3}
10^{-2}
x
10^{-1}
1

Fig. 8

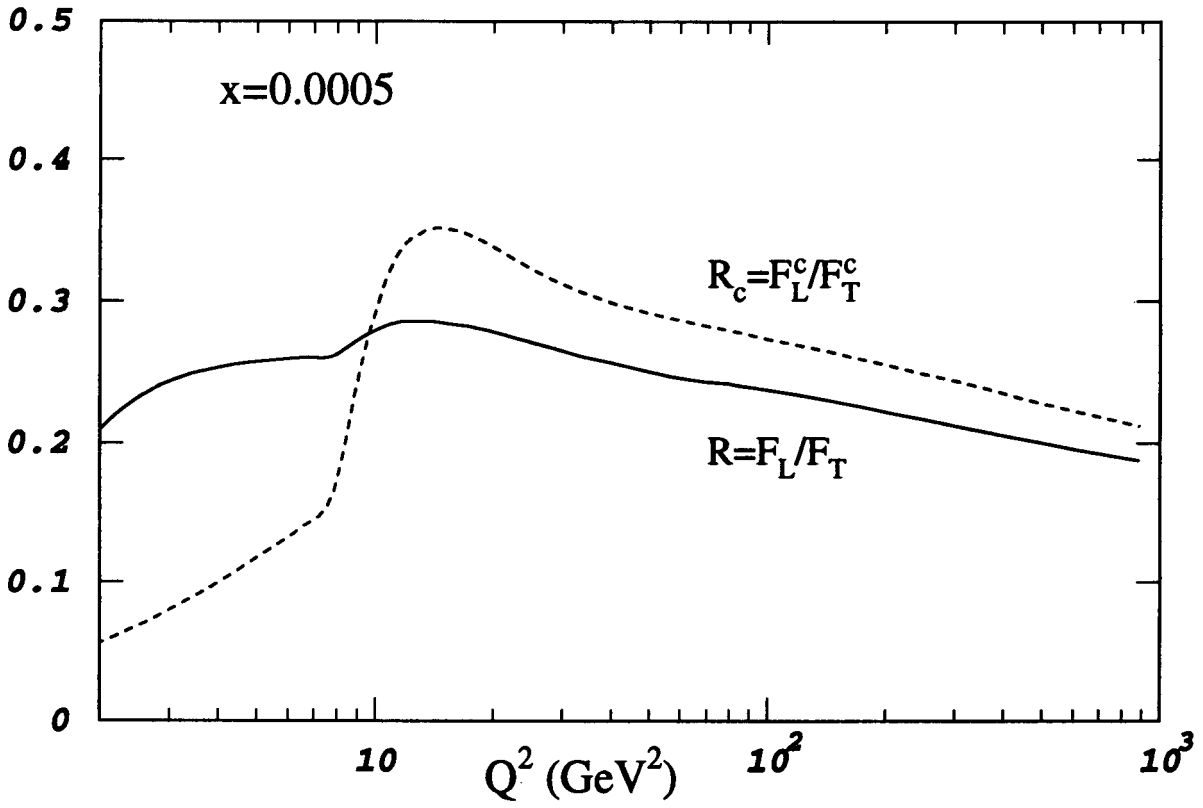
0.5
0.4
0.3
0.2
0.1
0
x=0.0005
$R_c=F_L^c/F_T^c$
$R=F_L/F_T$
10
Q^2 (GeV^2)
10^2
10^3

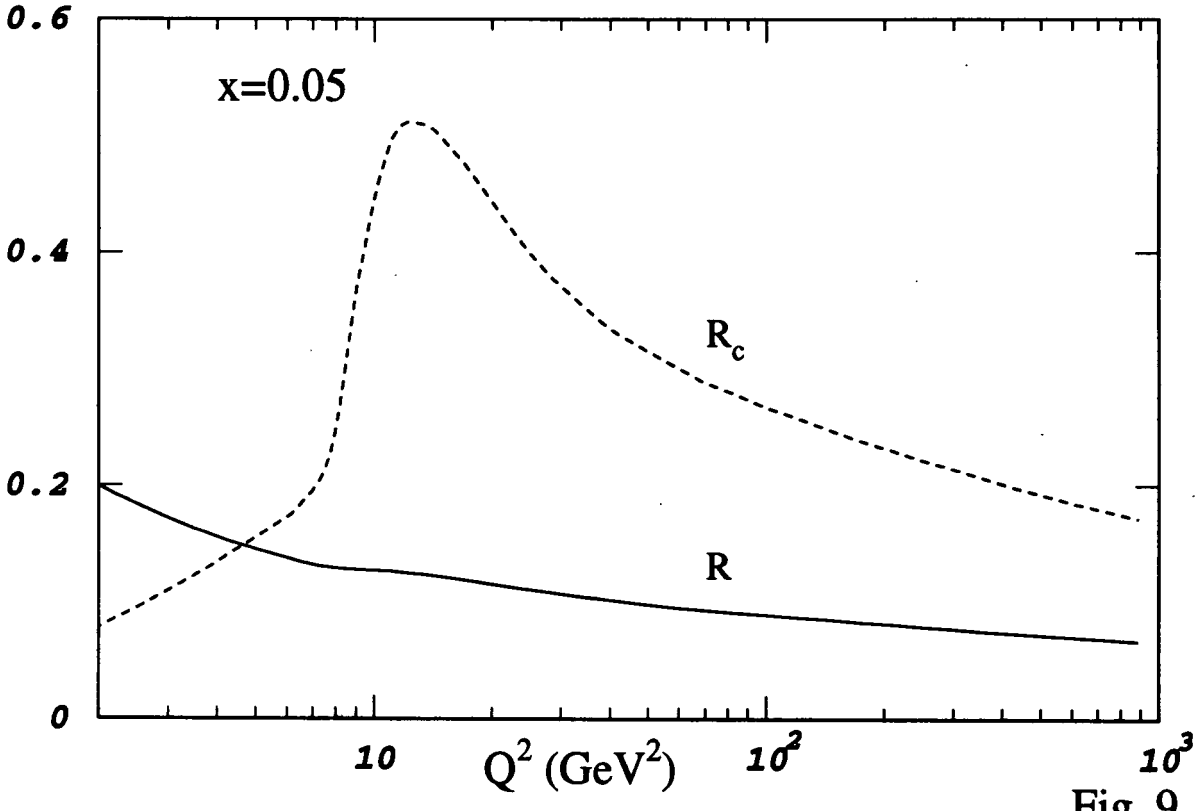
0.6
0.4
0.2
0
x=0.05
R_c
R
10
Q^2 (GeV^2)
10^2
10^3

Fig. 9